Catalytic performance of copper supported on zirconia polymorphs for CO hydrogenation

Zhong-Yi Ma, Cheng Yang, Wei Wei, Wen-Huai Li, Yu-Han Sun*

State Key Laboratory of Coal Conversion, Institute of Coal Chemistry, Chinese Academy of Sciences, Taiyuan 030001, PR China

Abstract

Cu/ZrO_2 catalysts with amorphous, monoclinic and tetragonal zirconia as supports were prepared and characterized by XRD, H_2-TPR, N_2O-titration, FT-IR and CO hydrogenation techniques. It was found that zirconia polymorphs had a great influence on the interaction of Cu and ZrO_2. Though it had the lowest surface area, tetragonal zirconia supported copper catalyst showed the highest copper dispersion and the best catalytic performance for methanol synthesis from CO hydrogenation. The formate and methoxyl species were evidenced as intermediates by FT-IR in the case of CO hydrogenation, and the formate-to-methoxyl mechanism was suggested for methanol synthesis on Cu/ZrO_2 catalyst.
© 2004 Elsevier B.V. All rights reserved.

Keywords: Zirconia polymorphs; Cu/ZrO_2; FT-IR; Methanol synthesis

1. Introduction

Cu/ZrO_2 catalysts showed interesting catalytic behavior for CO and CO_2 hydrogenation [1]. Zirconia by itself was a catalyst for the synthesis of methanol, in contrast to SiO_2 and Al_2O_3 and, in addition, it provided adsorption sites for formation of surface intermediates. Furthermore, Cu/ZrO_2 catalyst exhibited mechanical stability, a moderately high specific surface and good semiconducting properties. Mechanistic studies of methanol synthesis have demonstrated that zirconia played an important role in CO/CO_2 hydrogenation. The high catalytic activity of Cu/ZrO_2 was unanimously ascribed to the special active sites, but the precise role of these active sites was difficult to understand and still controversial in the literature. Shibata et al. [2] and Baiker et al. [3] proposed that copper was incorporated in zirconia with high surface area, and the decrease of the methanol synthesis rate was due to the crystallization of the initial amorphous zirconia. For the sol–gel derived Cu/ZrO_2 catalyst, Sun [4,5] found

that strength and nature of the interaction between dispersed copper and zirconia rather than surface area was decisive for CO/CO_2 hydrogenation. Furthermore, Chen et al. [6] claimed that the high activity of Cu/ZrO_2 might be attributed to copper to zirconia electron transfer. In situ FT-IR results showed that the formate and methoxyl species formed on zirconia for CO/H_2 adsorption on ZrO_2/SiO_2 or $Cu/ZrO_2/SiO_2$ [7]. The presence of Cu greatly accelerated the hydrogenation of formate to methoxyl species. Therefore, methanol synthesis over $Cu/ZrO_2/SiO_2$ was envisioned on zirconia, and the spillover of the species activated on copper to zirconia was critical to methanol synthesis activity.

Other controversy concerning the nature of the surface intermediates which was pivotal to the formation of methanol was well known. Indeed, for most of authors, the formate species was the precursor of methanol, whereas for other authors, this pivotal species was the bidented carbonate, which was directly hydrogenated to the methoxyl species. On the basis of various studies of CO hydrogenation, as well as the reaction of syngas on pure zirconia and zirconia-supported catalysts, Ekerdt et al. [8,9] proposed a low temperature mechanism in which formate was hydrogenated to

* Corresponding author. Tel.: +86 351 4049612; fax: +86 351 4041153.
  E-mail address: yhsun@sxicc.ac.cn (Y.-H. Sun).

dioxymethylene, which could either further react with hydrogen, producing the methane, or be desorbed as methanol in the presence of water. Wokaun et al. [10,11] found that π-bonded formaldehyde, which was formed during the catalytic reaction of CO hydrogenation, was the key intermediate. Subsequent reduction yielded surface-bound methylate and methanol.

At the same time, zirconia was claimed to exhibit three different polymorphs, and the phase structure of zirconia was important for many materials and catalytic reactions. Jung and Bell [12] reported that Cu/ZrO$_2$ catalysts with tetragonal and monoclinic zirconia as supports exhibited different activity for methanol synthesis from both CO and CO$_2$ hydrogenation. And He et al. [13] found that the tetragonal zirconia exhibited a high activity to form ethanol and the monoclinic zirconia showed high activity to form *iso*-butanol.

However, there was little report about the effect of zirconia polymorphs on Cu–ZrO$_2$ interaction and copper state and then on the relationship between active sites and methanol synthesis from CO hydrogenation. In this work, amorphous, monoclinic and tetragonal zirconia supported copper catalysts were prepared and then characterized by XRD, H$_2$-TPR, N$_2$O-titration and FT-IR techniques, and the catalytic performance of methanol synthesis from CO hydrogenation were also investigated.

2. Experimental

2.1. Catalysts preparation

Samples were prepared by impregnating different zirconia polymorphs with Cu(NO$_3$)$_2$ solution of the desired concentrations and then dried and calcined at 623 K for 3 h. Copper content was 10 wt.%, and the density of catalysts was about 1.3 g/ml. Amorphous zirconia (am-ZrO$_2$) was prepared from a solution of oxychloride zirconium co-precipitation with ammonia. After aging in the mother liquid for 3 h, the gel was filtered with distilled water until chloride test negative for AgNO$_3$ and then dried and calcined at 623 K for 3 h. The precipitate prepared as above aged for 5 days in the mother liquid at 323 K, and then dried and calcined at 823 K for 3 h, monoclinic zirconia (m-ZrO$_2$) could be obtained. Tetragonal zirconia (t-ZrO$_2$) was prepared by co-precipitating a solution of oxychloride zirconium with sodium carbonate, followed similar filtering and drying to am-ZrO$_2$ and m-ZrO$_2$, and then precipitate was calcined at 823 K for 3 h.

2.2. Characterization of catalysts

The specific surface areas of the catalysts were measured using Tristar 3000 Chemical Adsorption Instrument. BET surface areas were calculated from the linear part of the BET plot, and pore size distribution was estimated from the adsorption branch of the isotherm by the method of Horvath and Kawazoe.

Powder X-ray diffraction (XRD) patterns were recorded on a Rigaku D/Max diffractorments equipped with a Cu target and Ni filter.

TPR runs were carried out in a U-tube quartz reactor at a heating rate of 10 K/min with a programmable temperature controller. A hydrogen-nitrogen mixture (containing 5 vol.% of hydrogen) was passed over 50 mg catalysts at a total flow-rate of 30 cm^3/min and hydrogen consumption was monitored by a thermal conductivity cell attached to a gas chromatograph. The effluent gas was passed through a cold trap placed before TCD in order to remove water from the exit stream of the reactor. The hydrogen consumption of various catalysts was calculated on the basis of the area of their TPR profiles and the profile of the standard sample of CuO.

The copper surface area (SCu) was determined by applying a nitrous oxide pulse method as described in the literature [14,15]. A catalyst sample was placed in a quartz tube reactor and reduced at 573 K for 4 h in flowing hydrogen. After reduction, the gas flow was switched to argon and the temperature was lowered to 353 K. A pulse of nitrous oxide was introduced into the argon flow by means of a calibrated sample valve. The exit gas was analyzed by mass spectrometer. Copper surface area was calculated from the amount of nitrogen evolved, assuming the dissociation of nitrous oxide takes place on surface copper (average atom density: 1.49×10^{19} atoms/m^2):

$$N_2O\,(g) + 2Cu_s = N_2\,(g) + (Cu{-}O{-}Cu)_s \qquad (1)$$
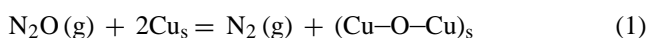
The diffuse reflectance FT-IR (DRIFT) method was described previously [16]. Spectra were recorded using Nicolet Magna-II 550 FT-IR spectrometer equipped with Spectra-Tech Diffuse Reflectance Accessory and a high temperature in situ cell with ZnSe windows. A KBr beam splitter has been used with a TGS detector. The catalyst was reduced in situ at 573 K for 4 h under atmospheric pressure by a stream of H$_2$. After switching to Ar, the sample was cooled down to 373 K and H$_2$/CO (2:1 mol) was introduced for 15 min. Thereafter, the system was cooled to the room temperature, swept with argon (99.99%) and collected the IR spectra. Then the temperature of system was increased to other desired value (between 373 and 573 K). Subsequently, the above-mentioned experiments procedure was applied again. Each spectrum was then referenced to a spectrum of the catalyst colleted at the room temperature under H$_2$ flow before adsorption CO/H$_2$, as appropriate.

2.3. Catalytic activity test

CO hydrogenation tests were carried out using a stainless steel fixed-bed reactor, which contained 1.0 ml catalyst. All catalysts were reduced in H$_2$ (5% in N$_2$) flow at 573 K and atmospheric pressure for 6 h before syngas exposure. Shimazu-8A GC was used to analyze the products. H$_2$, CO, CH$_4$ and CO$_2$ were determined by thermal conductivity detector (TCD) equipped with a TDX-101 column. Water and methanol in liquids were also detected by TCD with a GDX-

401 column. The alcohols and hydrocarbons were analyzed by flame ionization detector (FID) with a Propake-Q column.

3. Results and discussion

3.1. Textural and structural properties

Three catalysts exhibited large differences in BET surface area, pore volume and pore size (see Table 1). The BET surface area of Cu/am-ZrO$_2$ catalyst was as high as 147.9 m^2/g with the pore volume of 0.14 cm^3/g. Cu/m-ZrO$_2$ catalyst had the largest pore size and moderate surface area and pore volume. The BET surface area of Cu/t-ZrO$_2$ catalyst was only 24.5 m^2/g. These differences might be associated with zirconia polymorphs.

Fig. 1 shows the XRD patterns of three Cu/ZrO$_2$ catalysts. Zirconia polymorphs hardly changed after impregnating copper. The diffraction peaks of monoclinic or tetragonal zirconia were predominant for Cu/m-ZrO$_2$ and Cu/t-ZrO$_2$ catalysts. Two weak diffraction peaks of copper oxide were observed on Cu/m-ZrO$_2$ catalyst at 25.5° and 38.8°. But for Cu/t-ZrO$_2$ catalysts, diffraction peaks of copper oxide were hardly detected, which indicated that the copper dispersion on Cu/t-ZrO$_2$ catalyst was highest among three catalysts, and copper oxide particles might disperse highly on the catalyst surface.

Copper dispersion and surface area determined from N$_2$O-titration were also listed in Table 1. Cu/m-ZrO$_2$ catalyst exhibited the smallest copper surface and dispersion, which was in line with the XRD results. While for Cu/t-ZrO$_2$ catalyst, the copper dispersion and surface area were the highest though it
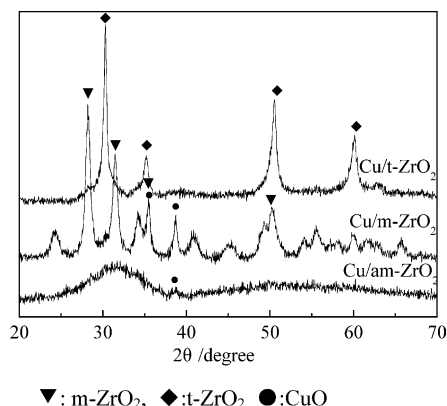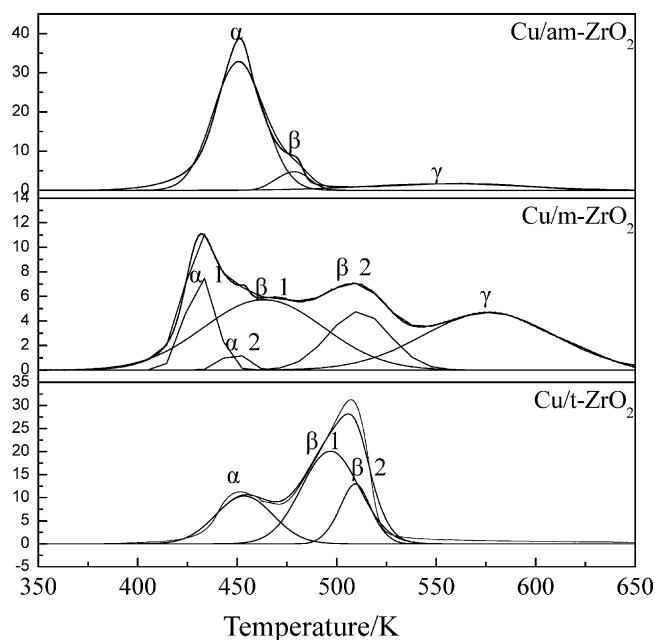

Fig. 2. H$_2$-TPR curves of three Cu/ZrO$_2$ catalysts.

had smallest surface area. These differences might originate from the different surface properties of zirconia polymorphs. Hertl [17] suggested that zirconia polymorphs showed different acid–base properties: tetragonal zirconia possessed high basicity while monoclinic zirconia and amorphous zirconia had relative high acidity. During catalysts preparation, surface properties of zirconia polymorphs impacted the interaction between Cu^{2+} and zirconia. Copper could be dispersed highly on the relative basicity surface, and resulted in the higher copper surface area of Cu/t-ZrO$_2$ catalyst.

3.2. Reduction behavior

The TPR curves of catalysts were shown in Fig. 2. For quantitative analysis, all of the peaks that could be deconvoluted by a Gaussian-type function were integrated to evaluate their individual amounts (see Table 2). Three peaks could be

▼: m-ZrO$_2$, ◆:t-ZrO$_2$ ●:CuO

Fig. 1. XRD patterns of three Cu/ZrO$_2$ catalysts.

Table 2
H$_2$ consumption estimated by H$_2$-TPR

Catalysts	H$_2$ consumption (mmol H$_2$ × 10^{-2})			
	α1	β1	γ	Total
Cu/am-ZrO$_2$	6.12	0.57	0.98	7.67
Cu/m-ZrO$_2$	1.02	3.80	2.38	7.20
Cu/t-ZrO$_2$	2.11	5.64	–	7.75

Table 1
Textural and structural of three Cu/ZrO$_2$ catalysts

Catalysts	S_{BET} (m^2/g)	V_P (cm^3/g)	Pore size (nm)	S_{Cu}[a] (m^2/g)	Cu dispersion[a] (%)
Cu/am-ZrO$_2$	147.9	0.14	3.1	3.9	2.3
Cu/m-ZrO$_2$	38.2	0.12	13.1	3.5	2.1
Cu/t-ZrO$_2$	24.5	0.04	5.1	4.6	2.7

[a] Determined from N$_2$O-titration.

seen at 452 K (referred to as peak α), 470 K (peak β, a shoulder of α) and 579 K (peak γ) for Cu/am-ZrO$_2$ catalyst. The hydrogen consumption of α peak was several times higher than that of β and γ peaks, and the peaks α and β temperature were lower compared to the peak γ temperature. Hence, the reduction of α and β peaks seemed to be the extrinsic behavior of copper oxide. Shimokawabe et al. [18] have demonstrated that the low temperature peak centered at 490 K was due to the reduction of highly dispersed cupric oxide and/or isolated Cu^{2+} ions in an octahedral environment, while the high temperature one corresponding to the range of 520–570 K ascribed to reduction of the bulk-like copper oxide. Therefore peaks α and β were ascribed to the reduction of highly dispersed cupric oxide clusters and/or the isolated copper ion with strong or weak interaction with support, while the γ peak was ascribed to reduction of the bulk CuO.

It was interesting to note that five peaks at 431 K (peak α1), 452 K (peak α2), 470 K (peak β1), 507 K (peak β2) and 579 K (peak γ) were obtained during the reduction of Cu/m-ZrO$_2$ catalyst. Zhou [19] ascribed the α and β peaks to the reductions of highly dispersion copper species whereas γ peak was attributed to the reduction of bulk copper oxide. Dow et al. [20] found two low temperature peaks below 450 K when copper oxide supported on yttrium-stabilized zirconia (YSZ). The reduction peaks were contributed to the hydrogen consumption of weakly bonded oxygen ions of copper oxide located on and beside the surface oxygen vacancies of YSZ support. According to the integrated results of TPR peaks shown in Fig. 2 and hydrogen consumption listed in Table 2, the peaks α1 and α2 of Cu/m-ZrO$_2$ catalyst were related to the surface oxygen vacancies of monoclinic zirconia with special geometry structure. At the same time, two β peaks were ascribable to the reduction of highly dispersion copper species with different environment or interaction with monoclinic zirconia support, and the γ peak could be contributed to the reduction of bulk copper oxide.

Cu/t-ZrO$_2$ showed three peaks at 451 K (peak α), 495 K (peak β1), and 507 K (peak β2), and no γ peak could be seen. The β1 peak temperature was higher than that of Cu/m-ZrO$_2$ catalyst, indicating that some copper species on Cu/t-ZrO$_2$ was difficult to be reduced. XRD pattern and N$_2$O-titration showed copper was dispersed highly on Cu/t-ZrO$_2$ catalyst. Hence, the interaction of copper with zirconia was intimate, which impacted the reduction of copper oxide. Similar to the above, the peaks α and β might be related to the reduction of highly dispersion copper species with different environment and interaction with zirconia. And the absence of reduction of bulk copper oxide also implied the highly dispersed copper on Cu/t-ZrO$_2$ catalyst.

In fact, from a point of catalysis, the reduction of CuO could be viewed as an autocatalytic process after experiencing an initial induction period during which hydrogen molecule was activated [21]. It was reported that a large concentration of defects in the oxide would lead to a decrease in the induction time. Being p-type semiconductor, zirconia possessed abundant oxygen defects and, therefore, an inti-

mate contact between copper and zirconia might facilitate H$_2$ activation, an important step required for the copper reduction. Hence, the reduction performances of Cu/ZrO$_2$ catalyst were largely related to the surface properties of zirconia supports, which possessed varied surface properties and had great influence on copper oxide environment and interaction with zirconia. Successively, influence on the formation of different copper oxide species was evidenced by the different reduction performance of three Cu/ZrO$_2$ catalysts.

3.3. DRIFT spectra of CO/H$_2$ adsorption

Fig. 3 shows the reaction of CO/H$_2$ on three Cu/ZrO$_2$ catalysts as a function of adsorption temperature. When syngas adsorbed on Cu/am-ZrO$_2$ catalyst at 373 K, a CO band at 2120 cm^{-1} was detected and red-shifted to 2113 cm^{-1} when reaction temperature changed from 373 to 573 K, while the intensity changed little, which reflected that the surface copper state changed slightly as a function of reaction temperature. In addition, the bicarbonate and carbonate species with the bands at 1619, 1554, 1360 and 1320 cm^{-1} were observed. Simultaneously, the formate species with the characteristic bands at 1577 and 1377 cm^{-1} was detected. After syngas adsorbing on Cu/am-ZrO$_2$ catalyst at 523 K for 15 min, besides the formate species, a new peak located at 1157 cm^{-1} was detected, which was ascribed to the rocking vibration of C–H species [11], indicating that the methoxyl species was formed at 523 K. Other bands of methoxyl species also could be found when reaction temperature reached 573 K. The symmetric and antisymmetric stretching vibrations of the CH$_3$ group at 2930 and 2823 cm^{-1}, the symmetric deformational motion of CH$_3$ group at 1465 cm^{-1}, and the C–O stretching bands at 1049 cm^{-1} were obviously appeared.

In the case of CO/H$_2$ reaction over Cu/m-ZrO$_2$ catalyst, CO band behaved similarly to CO adsorption on Cu/am-ZrO$_2$ catalyst as temperature changing. The intensity of CO band decreased as a function of reaction temperature, while it enhanced when reaction temperature reached 573 K. CO disproportionation was reported to occur on the surface of the catalyst, i.e. $2CO \rightarrow C + CO_2$. The graphite carbon deposited on the active sites, which then enshrouded the CO adsorption and resulted in the decrease of band intensity. TPR results showed that the copper species on Cu/m-ZrO$_2$ catalyst had complicated environment and interaction with monoclinic zirconia. Below 573 K, the copper oxide on Cu/m-ZrO$_2$ catalyst could not be reduced entirely. Hence, with the temperature increasing, syngas reacted with copper oxide and then caused the further reduction of copper oxide, which then caused the increase of CO band at 573 K. On the other hand, the formate species with band at 1573 and 1370 cm^{-1} was detected and became the major species even at 373 K, these may be contributed to the abundant surface hydroxyl on monoclinic zirconia [22]. The intensity of formate species became strong and then reached the maximum as the temperature increasing. At the same time, the methoxyl species with bands at 2930, 2827, 1153 and 1049 cm^{-1} appeared when the temperature
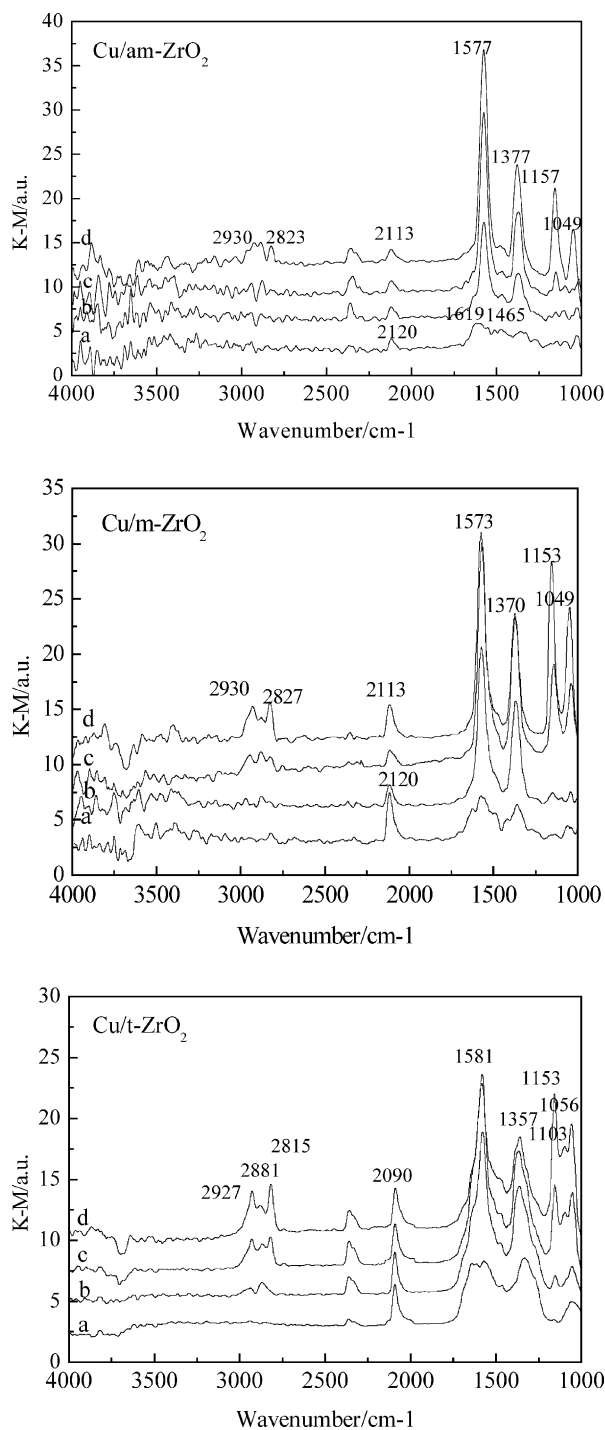
Fig. 3. Difference DRIFT spectra of CO/H_2 adsorption on three Cu/ZrO_2 catalysts as a function of temperature: (a) 373 K; (b) 473 K; (c) 523K; (d) 573 K.

reached 523 K. As the temperature increased further, the intensity of formate peaks decreased and the methoxyl peak enhanced largely (see Table 3). The decrease of formate species could be explained by the transformation of formate to methoxyl species under hydrogen atmosphere at high temperature, which also could be evidenced by the enhancement of the methoxyl species.

When syngas adsorbed on $Cu/t-ZrO_2$ catalyst, the behavior behaved differently to those of two former catalysts. CO band located at $2090\,cm^{-1}$ without red shift was detected, indicating large difference in copper state on $Cu/t-ZrO_2$ catalysts. This was in accordance with the TPR results that copper oxide could be thoroughly reduced above 573 K on $Cu/t-ZrO_2$ catalyst. CO bound on metallic copper had been shown to manifest stretching frequencies typically below $2110\,cm^{-1}$. The band of CO adsorption on Cu^+ sites has been reported between 2110 and $2135\,cm^{-1}$ [23]. Therefore, the metallic copper species existed on $Cu/t-ZrO_2$ catalyst and the Cu^+ species or some $Cu^{\delta+}$ species ($\delta+$ refer to the charge between 0 and +1) appeared on $Cu/am-ZrO_2$ and $Cu/m-ZrO_2$ catalysts. Another difference for $Cu/t-ZrO_2$ catalyst was the CO_2 band appeared at about $2356\,cm^{-1}$, which was stronger than that of other two catalysts. Carbonate and formate species with bands at 1640, 1370, 1460, and $1330\,cm^{-1}$ also appeared at 373 K, while carbonate species with a shoulder at $1640\,cm^{-1}$ was hardly disappeared even at 573 K. These might be corresponding to the properties that tetragonal zirconia possessed enhanced capacity of formation carbonate species [24]. It was interesting to note that methoxyl species with bands at 1153 and $1056\,cm^{-1}$ was detected even at 473 K (see Fig. 3), which appeared at lower temperature compared to other two catalysts. The formate species was enhanced at elevated temperature and then hydrogenated to methoxyl species with temperature increasing further, as proved by the decrease of formate species at 573 K. In the region of $1200–1000\,cm^{-1}$, besides the methoxyl species bands at 1153 and $1056\,cm^{-1}$, a shoulder band located at $1103\,cm^{-1}$ was observed. This band also could be attributed to another type of C–O vibration of methoxyl species, which reflected the complex methoxyl species formed on $Cu/t-ZrO_2$ catalyst.

Table 3 listed the absolute intensity of the HCOO and CH_3O species during CO hydrogenation as a function of reaction temperature. In the case of $Cu/am-ZrO_2$ catalyst, the intensity of formate species increased as the temperature increasing. While for $Cu/m-ZrO_2$ and $Cu/t-ZrO_2$ catalysts, the intensity of formate showed a maximum at 523 K, and then decreased with the rise of reaction temperature. The decrease could be explained by the conversion formate to methoxyl species. This difference also suggested that the conversion of formate to methoxyl on $Cu/am-ZrO_2$ catalyst was lower than that on other two catalysts. The intensity of HCOO species on

Table 3
The absolute intensity of CO, HCOO and CH_3O species on Cu/ZrO_2 catalysts as a function of temperature

Temperature (K)	HCOO			CH_3O		
	A	B	C	A	B	C
373	–	3.82	5.07	–	–	–
473	10.54	14.21	13.08	–	–	1.07
523	18.99	20.60	14.27	2.71	8.06	5.69
573	23.85	18.34	11.65	9.90	15.64	10.11

A: $Cu/am-ZrO_2$; B: $Cu/m-ZrO_2$; C: $Cu/t-ZrO_2$. Calculated from the band of IR spectra.

Table 4
Catalytic performances of three Cu/ZrO_2 catalysts

Catalysts	CO conversion (%)	Yield (g ml^{-1} h^{-1})	TOF	Carbon selectivity (%)[a]	
				HC[b]	ROH
$Cu/am-ZrO_2$	11.30	0.11	2.86	25.31	74.69
$Cu/m-ZrO_2$	9.28	0.07	2.64	20.13	79.87
$Cu/t-ZrO_2$	13.96	0.22	3.05	7.38	92.62

Reaction conditions: $T = 573$ K, $P = 8.0$ MPa, GHSV = 5000 h^{-1}, $H_2/CO = 2.0$.
  [a] Selectivity based on number of atoms per gram carbon = [number of CO converted to given product/total number of CO converted] × 100%.
  [b] HC: hydrocarbons.

$Cu/m-ZrO_2$ catalyst was higher than that of $Cu/t-ZrO_2$ when reaction temperature was above 373 K. And this was also the course in the intensity of CH_3O. Above 523 K, the intensity of CH_3O was almost two times higher on $Cu/m-ZrO_2$ than on $Cu/t-ZrO_2$ catalyst. These differences were attributed to the abundant surface hydroxyl and higher Lewis acidity/basicity of Zr^{4+}/O^{2-} pairs presented on the surface of monoclinic zirconia.

3.4. Catalytic performance

The activity and selectivity of CO hydrogenation over three Cu/ZrO_2 catalysts were listed in Table 4. $Cu/t-ZrO_2$ catalyst showed higher activity and selectivity to methanol synthesis from CO hydrogenation than the two other catalysts. The CO conversion and space-time yield were only 11.30%, 0.11 g/ml h and 9.28%, 0.07 g/ml h for $Cu/am-ZrO_2$ and $Cu/m-ZrO_2$ catalysts, respectively. The $Cu/t-ZrO_2$ catalyst was three times more active for methanol synthesis than that of $Cu/m-ZrO_2$ catalyst. On the basis of the data listed in Table 4 the conclusion could be made that tetragonal zirconia was the best support for methanol synthesis from CO hydrogenation compared to amorphous and monoclinic zirconia. These results were consistent with what He et al. [13] reported that the tetragonal phase showed better catalytic performance for CO hydrogenation compared to that of monoclinic phase. And He et al. [25] also examined the effect of reaction condition on the catalytic performance, but the results also showed that tetragonal phase had higher catalytic activity than that of monoclinic phase. While the present FT-IR results indicated that the intensities of HCOO and CH_3O species were stronger on $Cu/m-ZrO_2$ than on $Cu/t-ZrO_2$ catalyst.

In the case of mechanism for methanol synthesis from CO hydrogenation, the formate and methoxyl species were considered to be the intermediates. And the reaction proceeded from bidented formate via dioxomethylene and methoxyl to methanol. The required atomic hydrogen during the hydrogenation formate to methoxyl was rapidly formed by H_2 dissociated on copper, and the hydrogen spillover from copper to zirconia was more than an order of magnitude faster than the rate of methanol formation, and, hence, not a rate-limiting step in the synthesis of methanol over Cu/ZrO_2 [26]. Fisher and Bell [7] investigated the nature of the rate-limiting step in the methanol synthesis from CO hydrogenation by the

transient-response experiments. He deduced that the transformation of formate to methoxyl occurred more readily than that of methoxyl to methanol and that the latter reaction might be the difficult step along the route to gas-phase methanol. Methoxyl species could be eliminated by hydrogenation or hydrolyzation to methanol, while the latter case was rapider than the former [27]. The inconsistent of FT-IR spectra shown in Fig. 3 and Table 3 with the CO conversion and methanol space-time yield might be resulted from the influence of rate-limiting step in the case of methoxyl conversion to methanol. The water required during the hydrolyzation methoxyl to methanol could be produced by the reversed water gas shift reaction (RWGS), which occurred predominantly on the Cu surface, and this process was not affected significantly by the presence of zirconia. While the copper species was much affected by the zirconia polymorphs, confirmed by H_2-TPR and FT-IR, hence, zirconia polymorphs impacted effect indirectly on the RWGS reaction. The reaction of CO_2 and H_2 was conducted to determine the RWGS reaction on three copper catalysts at 573 K (see Fig. 4). It was found that the CO band on $Cu/t-ZrO_2$ catalyst was the strongest among three Cu/ZrO_2 catalysts. Therefore, combined with that in Fig. 3, the conclusion could be made that the RWGS reaction on $Cu/t-ZrO_2$ catalyst was strong and could supply more water to hydrolyze the methoxyl to methanol, subsequently, this catalyst exhibited the highest catalytic performance, though it showed weaker methoxyl band.
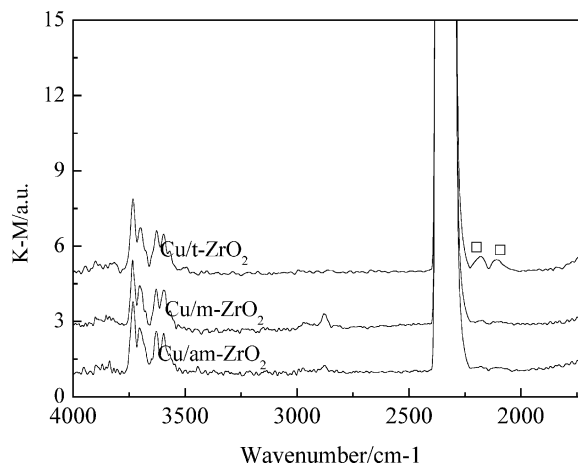

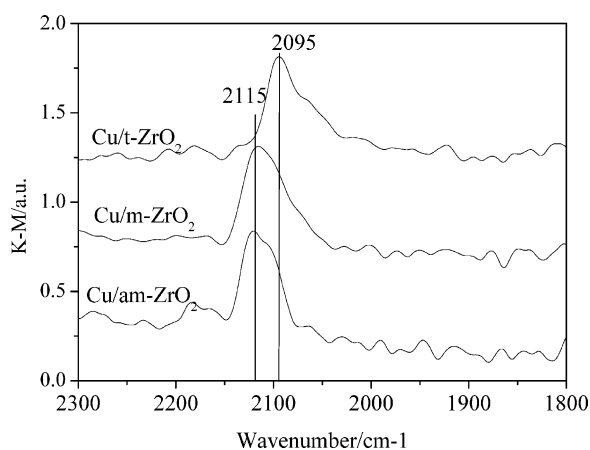Fig. 4. Difference DRIFT spectra of RWGS reaction on three copper catalysts at 573 K.

Fig. 5. Difference DRIFT spectra of CO adsorbed on three copper catalysts after removing reactants flow.

For methanol synthesis, Cu played an important role in the spillover of CO from Cu to ZrO_2 and in dissociating hydrogen to transform formate to methoxyl. Several possible active centers have been proposed including Cu^I [28,29] Cu^0–Cu^I [30,31] and copper metal [14,32]. In order to detect the influence of different zirconia polymorphs on the copper state and the ratio of Cu^0 and Cu^+, a new experiments of in situ CO-chemisorption after removing reactants flow (and products) was carried out. Different CO band was observed on three Cu/ZrO_2 catalysts (Fig. 5). The bands at 2115 and a shoulder at 2095 cm^{-1}, ascribed to CO adsorbed on Cu^+ and Cu^0, were detected on Cu/am-ZrO_2 and Cu/m-ZrO_2 catalysts. While almost no band at 2115 but at 2095 cm^{-1} was observed on Cu/t-ZrO_2 catalyst. These meant that the Cu^0 existed on three Cu/ZrO_2 catalysts while Cu^+ only existed on Cu/am-ZrO_2 and Cu/m-ZrO_2 catalysts. Based on the catalytic performance, the conclusion could be made that the Cu^0 species played an important role in the methanol synthesis from CO hydrogenation.

4. Conclusion

Zirconia polymorphs inflicted great difference on copper state and the reduction performance of copper oxide, which might originate from varied Cu–ZrO_2 interaction. The activity of methanol synthesis from CO hydrogenation on Cu/ZrO_2 was strongly influenced by the zirconia polymorphs. The methanol synthesis activity was higher for Cu/t-ZrO_2 than Cu/am-ZrO_2 and Cu/m-ZrO_2 catalysts. Based on the catalytic performance and FT-IR spectra, a conclusion could be made that the Cu^0 species played an important role in methanol synthesis from CO hydrogenation. The transformation of methoxyl to methanol was key step and the formate-to-methoxyl mechanism was observed.

References

[1] Y. Sun, P.A. Sermon, J. Chem. Soc., Chem. Commun. (1993) 1242.
[2] M. Shibata, Y. Ohbayashi, N. Kawata, T. Masumoto, K. Aoki, J. Catal. 96 (1985) 296.
[3] A. Baiker, M. Kilo, M. Macicjewshi, S. Menzi, A. Wokaun, New frontiers in catalysis, in: L. Guczi, et al. (Eds.), Proceedings of the 10th International Congress on Catalyst, Budapest, 1992, Elsevier, Amsterdam, 1993, p. 1257.
[4] G.S. Wu, Y.-H. Sun, Y.W. Li, et al., J. Mol. Struct. (2003) 287.
[5] Y.-H. Sun, P.A. Sermon, Catal. Lett. 29 (1994) 361.
[6] H.-W. Chen, J.M. White, J.G. Ekerdt, J. Catal. 99 (1986) 293.
[7] I.A. Fisher, A.T. Bell, J. Catal. 178 (1998) 153.
[8] M.-Y. He, J.M. White, J.G. Ekerdt, J. Mol. Catal. 30 (1985) 415.
[9] M.-Y. He, J.G. Ekerdt, J. Catal. 87 (1984) 238.
[10] J. Weigel, R.A. Koeppel, A. Baiker, A. Wokaun, Langmuir 12 (1996) 5319.
[11] C. Schild, A. Wokaun, A. Baiker, J. Mol. Catal. 63 (1990) 223.
[12] K.T. Jung, A.T. Bell, Catal. Lett. 80 (2002) 63.
[13] D. He, Y. Ding, H. Luo, C. Li, J. Mol. Catal. A 208 (2004) 267.
[14] J.W. Evans, M.S. Wainwright, A.J. Bridgewater, D.J. Young, Appl. Catal. 7 (1983) 75.
[15] R. Xu, Z.-Y. Ma, C. Yang, W. Wei, W.-H. Li, Y. Sun, J. Mol. Catal. A 218 (2004) 133.
[16] R. Xu, C. Yang, W. Wei, W.-H. Li, Y. Sun, J. Mol. Catal. A 221 (2004) 51.
[17] W. Hertl, Langmuir 5 (1989) 96.
[18] M. Shimokawabe, H. Asakawa, N. Takezawa, Appl. Catal. 59 (1990) 45.
[19] R.X. Zhou, T.M. Yu, X.Y. Jiang, F. Chen, X.M. Zheng, Appl. Surf. Sci. 148 (1999) 263.
[20] W.P. Dow, Y.P. Wang, T.J. Huang, J. Catal. 160 (1996) 155.
[21] J.A. Rodriguez, J.Y. Kim, J.C. Hanson, M. Pérez, A.I. Frenkel, Catal. Lett. 85 (2003) 247.
[22] K.T. Jung, A.T. Bell, J. Mol. Catal. 163 (2000) 27.
[23] A. Dandekar, M.A. Vannice, J. Catal. 178 (1998) 621.
[24] Z. Ma, R. Xu, C. Yang, W. Wei, Y.-H. Sun, Preprints of ACS Div. of Fuel Chem. 45 (2003) 193.
[25] D. He, Y. Ding, H. Yin, T. Wang, H. Luo, C. Li, Catal. Lett. 84 (2002) 89.
[26] K.-D. Jung, A.T. Bell, J. Catal. 193 (2000) 207.
[27] J. Wambach, A. Baiker, A. Workaun, PCCP 1 (1999) 5071.
[28] L.E.Y. Nonneman, V. Ponec, Catal. Lett. 7 (1990) 213.
[29] G.R. Apai, J.R. Monnier, M.J. Hanrahan, J. Chem. Soc., Chem. Commun. 212 (1984).
[30] J.A. Brown, Bourzutschky, N. Homs, A.T. Bell, J. Catal. 124 (1990) 52.
[31] Y. Okamoto, K. Fukino, T. Imanaka, S. Eranishi, J. Chem. Soc., Chem. Commun. (1982) 1405.
[32] G.C. Chinchen, K.C. Waugh, D.A. Whan, Appl. Catal. 25 (1986) 101.